



# Two new highly divergent and isolated *Madascincus* species from Nosy Be and the Tsingy de Namoroka, Madagascar (Squamata: Scincidae)

Aurélien Miralles<sup>1</sup>, Mark D. Scherz<sup>2</sup>, Sam Hyde Roberts<sup>3,4</sup>, Andolalao Rakotoarison<sup>5,6</sup>, Frank Glaw<sup>7</sup>, Miguel Vences<sup>8</sup>

1 Institut de Systématique, Évolution, Biodiversité (ISYEB), Muséum national d'Histoire Naturelle, CNRS, Sorbonne Université, EPHE, Université des Antilles, 57 rue Cuvier, 75231 Paris cedex, France

2 Natural History Museum Denmark, University of Copenhagen, Universitetsparken 15, 2100, Copenhagen Ø, Denmark

3 Duke University, Biological Sciences, Science Drive, Durham, North Carolina 27708, USA

4 SEED Madagascar, 7 Bell Yard, London, WC2A 2JR, United Kingdom

5 Mention Environnement, Université de l'Itasy, Faliarivo Ambohidanerana, 118 Soavinandriana Itasy, Madagascar

6 School for International Training, VN 41A Bis Ankazolava Ambohitsoa, Antananarivo, 101 Madagascar

7 Zoologische Staatssammlung München (ZSM-SNSB), Münchhausenstr. 21, 81247 München, Germany

8 Division of Evolutionary Biology, Zoological Institute, Braunschweig University of Technology, Mendelssohnstr. 4, 38106 Braunschweig, Germany

<https://zoobank.org/21F8A4B3-D34D-4DA6-8A7F-84A739352019>

Corresponding author: Aurélien Miralles (miralles.skink@gmail.com)

Academic editor Uwe Fritz

Received 27 October 2025

Accepted 9 February 2026

Published 6 March 2026

**Citation:** Miralles A, Scherz MD, Hyde Roberts S, Rakotoarison A, Glaw F, Vences M (2026) Two new highly divergent and isolated *Madascincus* species from Nosy Be and the Tsingy de Namoroka, Madagascar (Squamata: Scincidae). *Vertebrate Zoology* 76: 135–156. <https://doi.org/10.3897/vz.76.e176241>

## Abstract

*Madascincus* is a genus of quadrupedal skinks endemic to Madagascar, with 12 recognized species described between the 19<sup>th</sup> and 21<sup>st</sup> centuries, occupying diverse habitats from humid forests to arid southern regions and even high-altitude areas. Recent field expeditions uncovered two morphologically distinct forms that did not match any known species, prompting integrative taxonomic analyses that combine multilocus phylogenetics and morphology. Results revealed that each of these forms represents a highly divergent and likely ancient lineage, as evidenced by the substantial branch lengths in both mitochondrial and nuclear phylogenetic trees. These investigations led to the formal description of two new species with restricted distribution ranges: *Madascincus irery* **sp. nov.**, likely endemic to the island of Nosy Be, and *Madascincus minotaurus* **sp. nov.**, apparently restricted to the Tsingy de Namoroka karst system.

## Keywords

Biogeography, herpetofauna, integrative taxonomy, phylogeny, reptile, skink

## Introduction

*Madascincus* is a genus of fully quadrupedal skinks that belong to the endemic scincine clade that colonized Madagascar during the Paleogene period and successfully diversified on the island (Schmitz et al. 2005; Crottini et al.

2012; Miralles et al. 2022). Based on an integrative taxonomic revision combining multilocus and morphological datasets, Miralles et al. (2016) recognised a total of 12 described species within the genus, all endemic to Madagas-

car. Half of them (six) were described during the second half of the 19<sup>th</sup> century: *M. polleni* (Grandidier, 1869), *M. igneocaudatus* (Grandidier, 1867), *M. mouroundavae* (Grandidier, 1872), *M. melanopleura* (Günther, 1877), *M. stumpffi* (Boettger, 1882) and *M. macrolepis* (Boulenger, 1888). Two additional species were described during the 20<sup>th</sup> century: *M. ankodabensis* (Angel, 1930) and *M. minutus* (Raxworthy & Nussbaum, 1993). Finally, four species have been added in the 21<sup>st</sup> century: *M. nanus* (Andreone & Greer, 2002), *M. arenicola* Miralles, Köhler, Glaw & Vences, 2011, *M. pyrurus* Miralles, Köhler, Glaw & Vences, 2016, and *M. miafina* Miralles, Köhler, Glaw & Vences, 2016. Widely distributed across Madagascar and occupying a range of different biomes, species of the genus occur from the eastern humid evergreen forests (e.g., *M. melanopleura*) to the hottest and driest sandy areas of the South (e.g., *M. igneocaudatus*). One species, *M. pyrurus*, has even colonized the elevated and cool habitats of Mount Ibity (up to 1700 m a.s.l.).

During two field expeditions carried out in recent years, we had the opportunity to collect two forms of *Madascincus* that did not match any species previously recorded in the scientific literature morphologically. Their isolated geographical distribution, as well as the singular combination of morphological features they exhibit, prompted us to investigate the taxonomic status of these two forms more thoroughly using an integrative approach, combining multilocus phylogenetic analyses and morphological assessment, and we herein conclude that they represent new species, formally named and described in the taxonomy section below.

For the sake of simplicity and clarity, we anticipate our taxonomic results and introduce from here on their names. The first species, *Madascincus irery* **sp. nov.** was collected on Nosy Be, an island that covers an area of 321 km<sup>2</sup> and is located eight kilometers off the northwestern coast of Madagascar in the Sambirano region. The second species, *Madascincus minotaurus* **sp. nov.** was collected in the Tsingy de Namoroka, a labyrinthic karst system extending over ca. 220 km<sup>2</sup> and located within the Mahajanga basin in the North West of Madagascar.

## Materials and Methods

### Sampling, acronyms and definitions

In addition to the newly collected material, the comparative morphological dataset is composed of a total of 168 preserved specimens that were genotyped by Miralles and Vences (2013), complemented by 40 additional specimens without associated molecular data; as well as data previously published by Andreone and Greer (2002), Glaw and Vences (2007) and Miralles et al. (2011a, 2016). See File S1 for a complete list of the material examined. All the name-bearing type specimens known for this genus have been examined, except the types of *M. minutus* Raxworthy & Nussbaum, 1993 (UMMZ 192705) and *Sepsina vulsi-*

*ni* Barbour, 1918 (MCZ R-11869), regarded as a junior synonym of *M. melanopleura* (Günther, 1877), which are both unambiguously members of the *M. melanopleura* clade. The *Madascincus nanus* group is herein considered a putative assemblage of miniaturized species within *Madascincus* requiring formal taxonomic evaluation. It tentatively includes *M. nanus*, *M. macrolepis*, *Madascincus* sp. “baeus”, and a candidate species from Betampona. *Madascincus macrolepis* is excluded from most analyses due to its unresolved taxonomic status and the absence of molecular and recent voucher data.

Specimens are deposited in the Muséum National d’Histoire Naturelle, Paris (MNHN), Museo Regionale di Scienze Naturali, Torino (MRSN), Natural History Museum, London (NHMUK), Forschungsinstitut und Naturmuseum Senckenberg, Frankfurt am Main (SMF), Université d’Antananarivo, Département de Biologie Animale (UADBA), and Zoologische Staatssammlung München (ZSM). Where applicable, we provide their respective field numbers, belonging to each specimen, using the abbreviations: **FGZC**, **FGMV**, **MV**, and **MgF** referring to Frank Glaw, Miguel Vences and “Frontier, Madagascar” field numbers (cf. Suppl. material 1). Some specimens deposited at UADBA have not yet been formally catalogued in that collection, and we refer to these specimens as UADBA uncatalogued, followed by the respective field number (written on a tag physically attached to the specimens) to allow for unambiguous specimen identification. Abbreviations used for morphological traits are the following: **F**: frontal, **FN**: frontonasal, **IL**: infralabial, **IP**: interparietal, **L**: loreal, **M**: mental, **N**: enlarged nuchal, **O**: ocular, **P**: parietal, **PN**: postnasal, **PO**: preocular, **PoS**: postsubocular, **PrS**: presubocular, **PT**: pretemporal, **PS**: post-supralabial, **R**: rostral shield, **SL**: supralabial, **SN**: supranasal, **SO**: supraocular, **SVL**: snout–vent length, **1** and **2**: primary and secondary temporals. Geographic regions within Madagascar are named according to Boumans et al. (2007) and Brown et al. (2016).

### Morphological characters

The description of the two new species herein proposed involved recording meristic, mensural and categorical morphological characters routinely used in the taxonomy of Scincidae, such as scale counts, presence or absence of homologous scale fusions, or color patterns (cf. Andreone and Greer 2002; Miralles et al. 2011a, 2011b, 2011c, 2016). Ventral scales are counted in a single row from the postmental scales to the preanal scales, which both are included in the count, while the mental scale is excluded. The paravertebral scales are counted in a single row, starting from the first scale located immediately behind a line drawn perpendicular to the longitudinal axis of the body and connecting the posterior edges of the thighs, and continuing forward up to and including the nuchal scales. Nuchal scales (sensu Miralles 2006) are defined as enlarged scales of the nape, occupying transversally the place of two or more rows of dorsal cycloid scale. The frontal scale is considered hourglass-shaped when con-

stricted by the first supraocular, bell-shaped otherwise. Measurements of specimens were recorded to the nearest 0.1 mm using a dial caliper. Ranges are given for each meristic and mensural character, followed by the mean  $\pm$  the standard deviation, with sample size in parentheses. For some bilateral characters, the sample size has been noted as the number of sides rather than specimens (indicated after sample size).

## Molecular analysis

The de novo molecular dataset consists of eight sequences produced by Sanger sequencing for two individuals of the two new species under description. These sequences were combined with the extensive multilocus dataset previously published by Miralles and Vences (2013), which comprises six loci: two mitochondrial genes (16S rRNA, **16S**; and NADH Dehydrogenase Subunit 1, **ND1**) and four nuclear-encoded protein-coding genes (Brain-derived Neurotrophic Factor, **BDNF**; Recombination-Activating Gene 2, **RAG2**; Oocyte Maturation factor mos, **CMOS**; Phosducin, **PDC**). See Miralles and Vences (2013) for detailed descriptions of all the molecular procedures including primers and PCR protocols. We used Codon-Code Aligner 6.0.2 (CodonCode Corporation) to verify sequence quality of chromatograms and eliminate regions of poor read quality. New sequences were submitted to GenBank (accession numbers **PX853109** to **PX853114**, and **PX854599** to **PX854600**). The resulting data matrix is 98.5% complete, missing only 15 sequences from a possible total of 966; see File S2 for a detailed list of samples and GenBank accession numbers.

In total, three Bayesian inference (**BI**) phylogenetic analyses were carried out: (1) the main phylogenetic analysis involved the whole concatenated molecular dataset and was carried out using MrBayes 3.1.2 (Ronquist and Huelsenbeck 2003). Models of evolution were determined for each gene by AIC in MrModeltest 2.3 (Nylander 2004): GTR+G+I for ND1 and 16S rRNA, GTR+G for CMOS, K80+I for BDNF, K80+G for PDC, and HKY for RAG2. We performed one run of 10 million generations (started on random trees) and four incrementally heated Markov chains (using default heating values) each, sampling the Markov chains at intervals of 1000 generations. The first 2.5 million generations were conservatively discarded and 2500 trees were retained post burn-in and summed to generate a 50%-majority rule consensus tree. As hierarchical outgroups, we used *Flexiseps meva* and *Paracontias fasika*, the latter belonging to the sister clade of the genus *Madascincus* (Erens et al. 2017; Belluaro et al. 2023). Additionally, two complementary Bayesian analyses were carried out to detect possible mitonuclear phylogenetic discordance: (2) a BI combining only the four concatenated genes of the nDNA data set, and (3) another one combining only the two concatenated genes of the mtDNA data set. We relied on divergence estimates from already published time-calibrated phylogenetic trees (Miralles et al. 2015; Belluaro et al. 2023; Miralles et al. 2025).

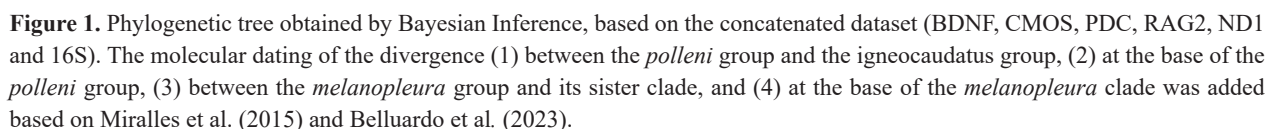
## Results

### Molecular analyses

The three Bayesian phylogenetic inferences (mtDNA, nDNA and mtDNA+nDNA) were congruent with each other and with previous studies focusing on *Madascincus*, in recovering five main clades which correspond to: (1) the *polleni* group (i.e., composed of *M. polleni*, *M. miafina*, *M. arenicola* and *M. stumpffi*), (2) the *igneocaudatus* group (*M. igneocaudatus* and *M. pyrusus*), (3) *M. mouroundavae*, (4) the *melanopleura* group (*M. melanopleura*, *M. minutus* and *M. ankodabensis*) and (5) the *nanus* group. In the same line, they also recovered the monophyly of a larger clade gathering the *polleni*, *igneocaudatus* and *mouroundavae* groups together, and the *nanus* group as the most basally connected branch of the genus tree (i.e., sister lineage to the clade comprising all the other species of *Madascincus* (Figs 1, 2A)).

In every analysis, the trees congruently retrieved the new lineages from Nosy Be and Namoroka as long branches deeply nested within the genus. *Madascincus irery* **sp. nov.** was retrieved, with relatively good support in both the combined and the mtDNA tree, as sister species of the *polleni* group (BI: 0.91 and 0.95, respectively). In contrast, its position is less resolved in the nDNA tree, as it is connected (with a weak support of 0.53) at a polytomous node, together with the *polleni* group, the *igneocaudatus* group, and *M. mouroundavae*. The uncorrected p-distances calculated between *Madascincus irery* **sp. nov.** and the *polleni* group ranged from 7.4% to 9.3% for the 16S gene and from 16.4% to 18.5% for the ND1 gene. *Madascincus minotaurus* **sp. nov.** was congruently retrieved in all analyses and with strong support (BI: 1.0 in both the all-marker tree and in the mtDNA tree, 0.93 in the nDNA tree) as sister species of the *melanopleura* group. The uncorrected p-distances calculated between *Madascincus minotaurus* **sp. nov.** and the *melanopleura* group ranged from 9.0% to 10.9% for the 16S gene and from 11.9% to 15.9% for the ND1 gene.

According to the topology obtained from the analysis of the all-marker dataset, it can be deduced that the ancestral lineage of *Madascincus irery* **sp. nov.** began to diverge after the differentiation between the *polleni* group and the *igneocaudatus* group, and before the diversification within the *polleni* group (Fig. 1). This represents an interval ranging between 26.9/24.6 million years (My) and 11.2/8.8 My according to Belluaro et al. 2023 and Miralles et al. 2015, respectively, which corresponds to the first half of the Miocene. Following the same rationale, the ancestral lineage of *Madascincus minotaurus* **sp. nov.** began to diverge after the divergence of the *melanopleura* group lineage, but before the diversification within that same group. This represents an interval ranging between 33.9/27.7 My and 24.9/16.0 My (also according to Belluaro et al. 2023 and Miralles et al. 2015, respectively) which corresponds to the Oligocene.



Morphological results are summarized in Table 1, and the most diagnostic traits are graphically represented in Figure 2B–D. *Madascincus irery* **sp. nov.** and *M. minotaurus* **sp. nov.** are both unambiguously diagnosable from all species of their respective sister clades (i.e., species of

the *polleni* group and species of the *melanopleura* group, respectively). More precisely, *Madascincus irery* **sp. nov.** is distinguishable from all the species of the *polleni* group (but also from *M. mouroundavae* and species of the *igneocaudatus* group) by a lower number of ventral scales, a dark and uniform colouration, a significantly smaller size and a very distinct head shape, characterized



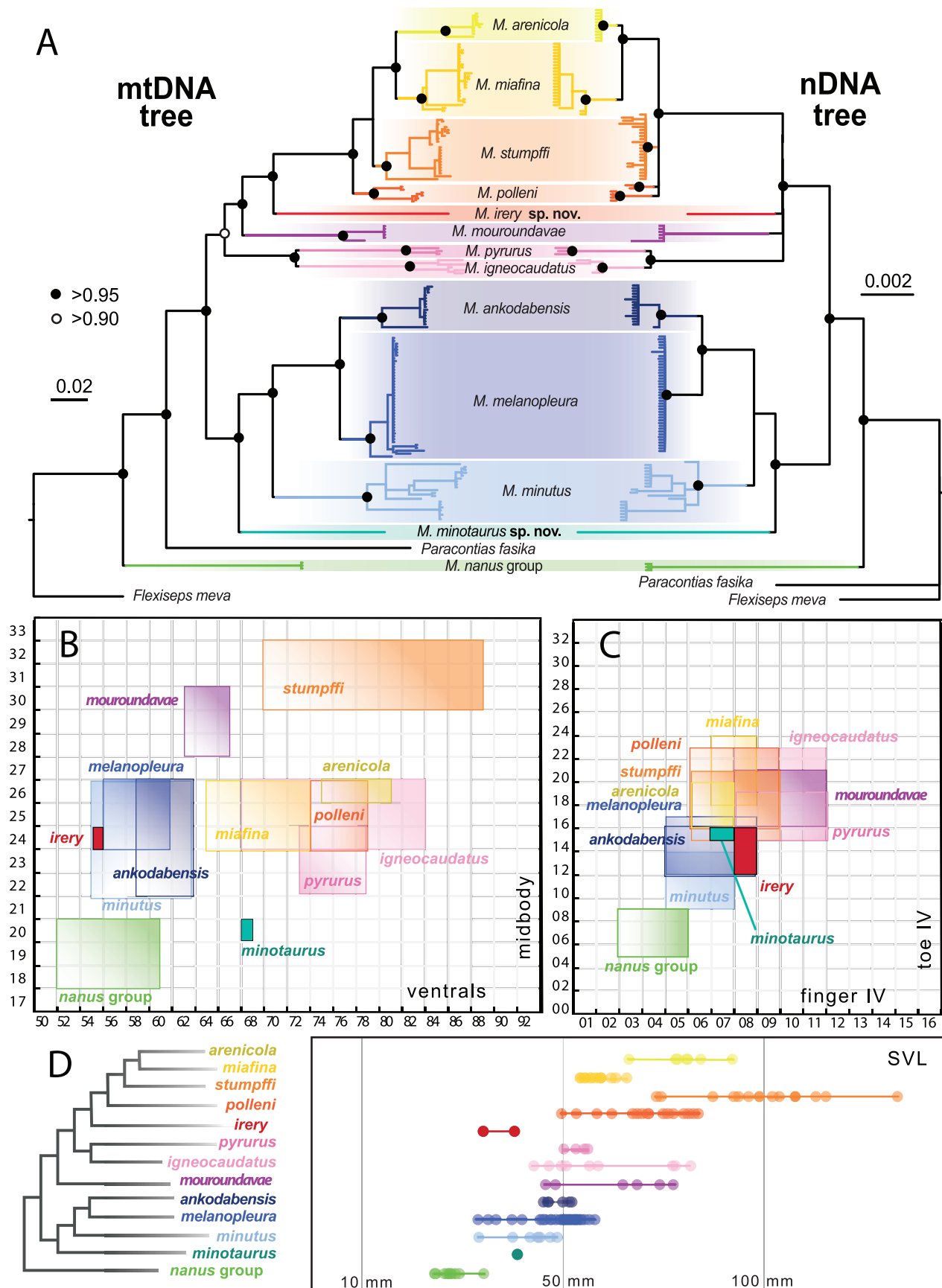


**Figure 2.** Molecular and morphological diversification within *Madascincus*. **A** Comparison of the phylogenetic trees based on nDNA (BDNF, CMOS, PDC and RAG2) and mtDNA (ND1 and 16S). **B–D** Graphical diagnosis of *Madascincus minotaurus* sp. nov. and *M. irery* sp. nov. displaying various morphospaces based on the ranges of intraspecific variation (min–max) of four traits: **B** Number of ventral scales and scale counts around midbody. **C** Number of subdigital lamellae on fourth fingers and fourth toes. **D** Comparison of the snout–vent length (SVL) variation for each species. Juvenile specimens have been removed, by using an arbitrary threshold (only specimens with SVL  $\geq 50\%$  of the maximum SVL value measured for each species were included).

by a rather short and pointed snout and large eyes. *Madascincus minotaurus* **sp. nov.** differs from the species of the *melanopleura* group by a higher number of ventral scales and a particular colouration pattern (see species diagnoses for more details).

This consistent morphological differentiation, in concert with isolated phylogenetic positions and high genetic divergences of the two new lineages unambiguously support their species status, and we therefore formally name and describe them in the following.

## Taxonomy

### *Madascincus minotaurus* **sp. nov.**

<https://zoobank.org/02B6EDA4-CC86-4BA9-9720-AADC-C7622D1E>

Figures 3–9

**Holotype.** MADAGASCAR – **Boeny Region** • 1 adult ♀; Tsingy de Namoroka National Park, Petit Tsingy; 16°26'7"S, 45°22'6"E; 125 m a.s.l.; 08 Oct. 2023, 07:00–09:00 a.m.; A. Miralles, N.A. Rahagalala, A. Rakotoarison, D. Razafimanafa and A. Razafimanantsoa leg.; ZSM 116/2023 (ZCMV 15819).

**Other material examined.** MADAGASCAR – **Boeny Region** • 1 tissue sample (MIRZC 1217, voucher not collected); Tsingy de Namoroka National Park, Grand Tsingy, south of the Tsingy massif, Camp 2; 16°28'9"S, 45°20'54"E, 128 m a.s.l.; 10 Oct. 2023, 03:00–07:00 p.m.; A. Miralles, N. A. Rahagalala, A. Rakotoarison, D. Razafimanafa and A. Razafimanantsoa leg. • 1 specimen photographed (unsampled and uncollected); Tsingy de Namoroka National Park, Grand Tsingy; 16°28'1"S, 45°21'0"E; photographed by Ivan Ineich on 3 Sept. 2012.

Furthermore, four specimens deposited in the UMMZ collection and registered as *Madascincus intermedius* (junior synonym of *M. polleni*) have been collected only 50 m from the sample MIRZC 1217. Given their collection locality and the superficial resemblance between *M. polleni* and *M. minotaurus* **sp. nov.**, we hypothesize that these specimens likely correspond to the new species: UMMZ 222106–222109, from Namoroka, camp 1, at the edge of Tsingy (16°28'11"S, 45°20'54"E); Dec. 1996; C.J. Raxworthy, J.B. Ramanamanjato, A. Razafimanantsoa and J. Rafanomezantsoa leg. These specimens/samples are not designated as paratypes because the specimens were not studied.

**Diagnosis.** *Madascincus minotaurus* **sp. nov.** differs from all other species in the genus *Madascincus* by the combination of a lower number of scales around midbody and a higher number of ventrals. It differs from the species of the *melanopleura* group (its sister clade formed by *M. melanopleura*, *M. ankodabensis* and *M. minutus*) by a distinctly higher number of ventrals (68, versus 55 to

63) and paravertebral scales (69, versus 51 to 65), by a bell-shaped frontal scale (versus hourglass-shaped, i.e., frontal constricted by the first pair of supraoculars) and a distinct, lighter and warmer coloration (versus darker and brownish).

**Description of the holotype.** (Figs 3, 4) An adult female, with a single large egg in the abdominal cavity. Good state of preservation, with exception of the left arm and the left leg that have been removed for molecular analyses. SVL (39.9 mm) 7 times head length (5.9 mm), almost as long as tail (41.0 mm, either entire or completely regenerated). Limbs very short, SVL 7.1 times forelimb length (5.5 mm) and 4.3 times hind limb length (8.9 mm). Snout short and rounded on lateral aspect, with a rostral tip bluntly rounded in dorsal aspect. Rostral wider than long, contacting first supralabial scales, nasals, and supranasal scales. Paired supranasal scales in median contact, contacting loreals and postnasal scales. Frontonasal scales roughly triangular, wider than long, contacting loreals, first supraciliaries and first supraoculars. Prefrontals absent. Frontal longer than wide, wider posteriorly, in contact with frontonasal, supraoculars, parietals and interparietal. Four supraoculars, all of them in contact with frontal; second pair larger than posteriormost pair; first pair not constricting frontal (frontal bell-shaped sensu Andreone and Greer 2002). Frontoparietals absent. Interparietal as long as wide, well separated from supraoculars; parietal eyespot present with parietal eye evident. Parietals contact posterior to interparietal. Two pairs of enlarged nuchals, each nuchal scale width corresponding to two transverse rows of adjacent cycloid scales. Nasals slightly larger than nostrils; contacting rostral, first supralabials, postnasals and supranasals. Postnasals present, separating supranasals from first supralabials, and nasals from loreals. Loreal single, slightly higher than long. Preocular trapezoidal, as long as high, single. Presubocular roughly square, single. Six supraciliaries on both sides, in continuous row; first and last pairs significantly larger than the intermediate ones; last pair projecting onto supraocular shelf. Pretemporals single, contacted by parietal. Two postsuboculars; upper contacting pretemporal; both contacting penultimate supralabial. Lower eyelid moveable, with a spectacted translucal window; lower palpebrals small, longer than high. Contact between upper palpebrals and supraciliaries seemingly direct but flexible, i.e., palpebral cleft narrow. Primary temporal single. Two secondary temporals; upper long, contacting pretemporal anteriorly and overlapping lower secondary temporal ventrally. Six supralabials, with the fourth being the enlarged subocular, contacting scales of the lower eyelid. External ear opening rounded, without lobules. Mental wider than long, posterior margin convex. Postmental wider than long, contacting first two pairs of infralabials. Six infralabials. Three pairs of large chin scales, both members of first pair in contact, both members of second pair separated by a single median scale, and members of third pair separated by three scale rows. No scales extending between infralabials and large chin scales. Gulars similar in size and outline to ventrals. All



**Figure 3.** Photos of *Madascincus minotaurus* **sp. nov.** in life. **A, B** Holotype ZSM 116/2023, from Tsingy de Namoroka National Park. **C** Uncollected specimen from Grand Tsingy. Photographs **A** and **B** by AM, **C** by Ivan Ineich.

scales, except head shields and scales on palms, soles, and digits, cycloid, smooth, and imbricate; 20 longitudinal scale rows at midbody; 69 paravertebrals, similar in size to adjacent scales; 68 ventrals. Inner preanals overlapped by outer. Both anterior and posterior limbs pentadactyl; fingers and toes relatively short, clawed, except the fifth finger which does not bear a claw; relative length of toes in the following order:  $I < II < III < V < IV$ . Subdigital lamellae smooth, single, with 7 under right fourth finger, 15 under right fourth toe.

**Coloration of the holotype.** In preservative, specimen with a pair of lateral dark brown stripes (about one scale wide on the neck), well defined anteriorly (overlapping rostral, mental, first four supralabials, loreals, and pre-suboculars), then progressively breaking up into a thin dashed lines posteriorly to forelimbs, hardly distinguishable from the rest of the dark dots covering the dorsum and the flanks. Presence on the anterior part of the body

of a pair of short light cream dorsolateral stripes, separating the dark lateral stripe from the bronze dorsal field, well-visible from supranasals, supraciliaries, temporal area and the neck to the level of the insertion of the forelimbs, but progressively fading and disappearing posteriorly. Dorsum and dorsal sides of forelimbs, hindlimbs and tail light bronze. The bronze dorsal field and the slightly lighter flanks are covered by numerous little dark dots, with each cycloid presenting a distinctive lunular at their insertion point and a cloud of tiny dark pigmentations at their middle, resulting in many thin dash lines (14 at midbody). No distinct border between the background coloration of the darker dorsal and the lighter ventral sides. Immaculate light cream ventral field extending from lower side of head (mental excluded), throat, lower side of limbs and venter, to ventral side of tail. Palms and soles greyish, darker than venter. In life, the coloration pattern was relatively similar to that in preservative, but with a slightly brighter and warmer overall aspect, evoking



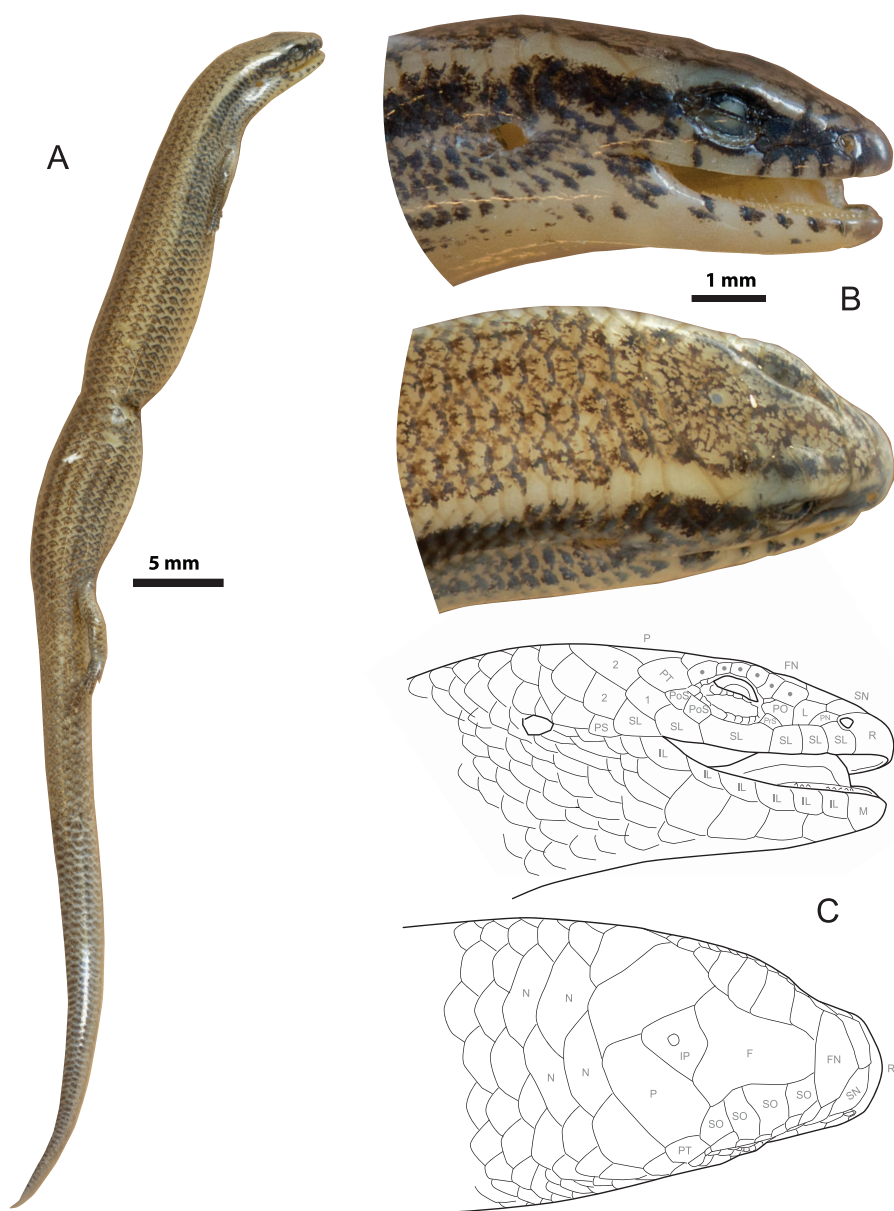


**Figure 4.** Preserved holotype of *Madascincus minotaurus* sp. nov., ZSM 116/2023, from Tsingy de Namoroka National Park. **A**, **B** photographs and **C** head drawings in lateral (above) and dorsal view (below). Abbreviations used in the drawings are explained in the Materials and Methods section.

more a copper than bronze background coloration. Light dorsolateral stripes on the head and the neck were more discernable and extending along the entire length of the body until hindlimbs insertion and presenting a brighter orange tint. Presence of slightly iridescent glints of scales (cf. Fig. 3A, B).

**Variation.** The only available additional information concerns a specimen photographed by Ivan Ineich at the Grand Tsingy; it presents a color pattern identical to that of the holotype (Fig. 3C).

**Etymology.** The specific epithet *minotaurus*, invariable noun in apposition, is derived from *Minótauros* (ancient Greek: Μινώταυρος), a taurine creature of the Greek mythology. It alludes to the labyrinthine structure of the Tsingy de Namoroka, within which the new species, like the Minotaur in Daedalus's construction, appears unable to escape.

**Distribution.** (Figs 5, 6, 9) Only known from the Tsingy area of the Namoroka National Park, North West of Madagascar, and probably distributed all over this karstic massif and surrounding patches of deciduous forest. The holotype was collected at the border of the Petit Tsingy (eastern part of the Namoroka massif), at the limit between the rock corridor and the adjacent dry deciduous forested area. The sample MIRZC 1217 was found on the border of the Grand Tsingy (southern part of the massif).

**Ecology.** The two specimens observed in 2023 were foraging in dense leaf-litter layers in shaded areas (by day) or active at dusk.

**Conservation status.** Considering that *Madascincus minotaurus* sp. nov. is likely widely distributed across the Namoroka karst massif, and based on satellite imagery, it is possible to conclude that its EOO might at least range from 50 to 200 km<sup>2</sup>, depending on whether the species



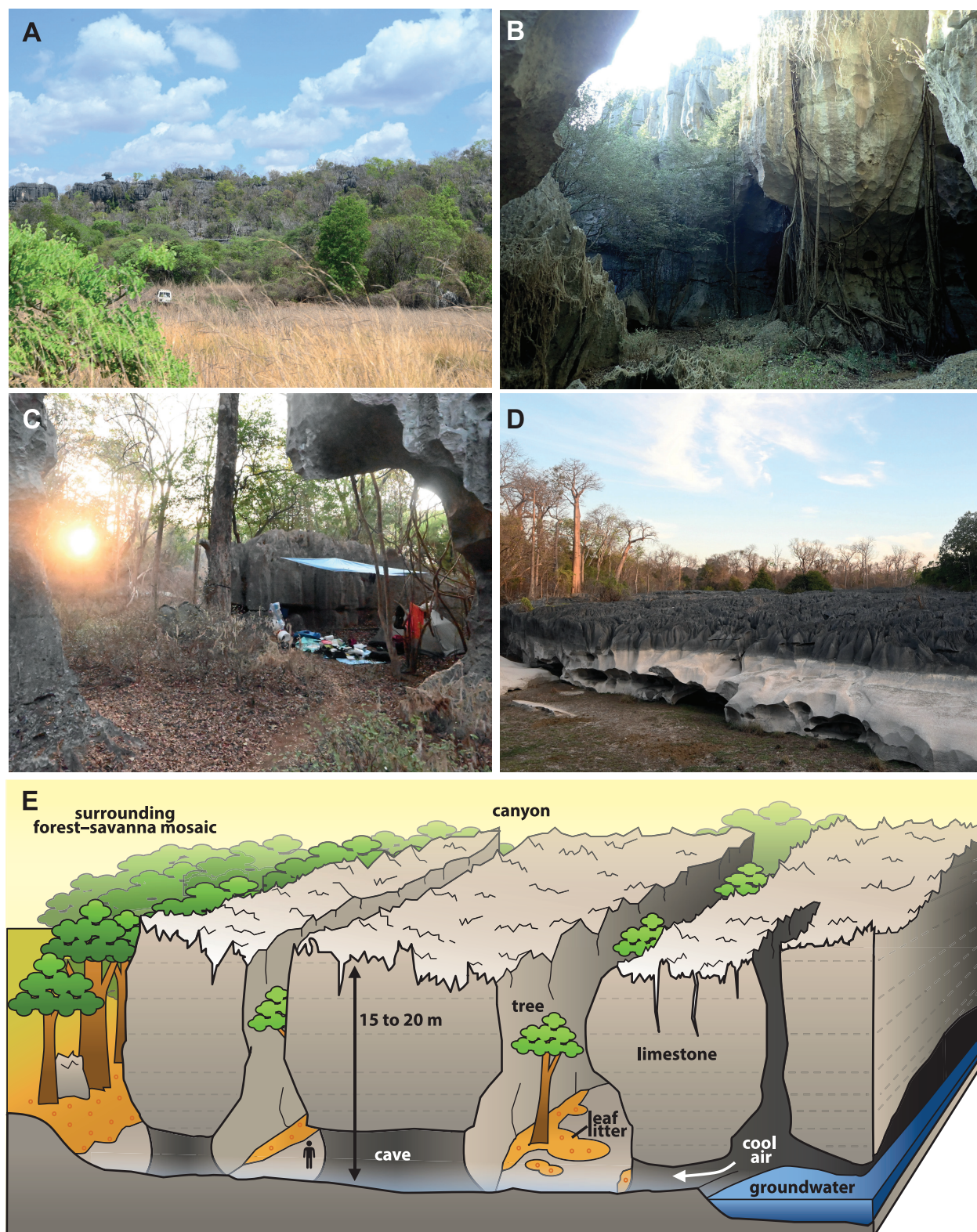


**Figure 5.** Habitat of *Madascincus minotaurus* sp. nov. at Tsingy de National Park. **A** View of the Grand Tsingy from the surrounding savanna. **B** View from inside a canyon at the Grand Tsingy. **C** Campsite at the border of Grand Tsingy, showing the leaf litter micro-habitat where the uncollected specimen (sample MIRZC 1217) was found. **D** Petit Tsingy, exact position of the type locality. **E** Diagram representing a transverse view of Grand Tsingy during the dry season (during the wet season, the depressed ground is heavily flooded). Specimens of *M. minotaurus* sp. nov. have been encountered in the leaf-litter located in the border of the karts system (corresponding to the orange surface on the left side of the diagram), although the species is likely present in the corridors too.



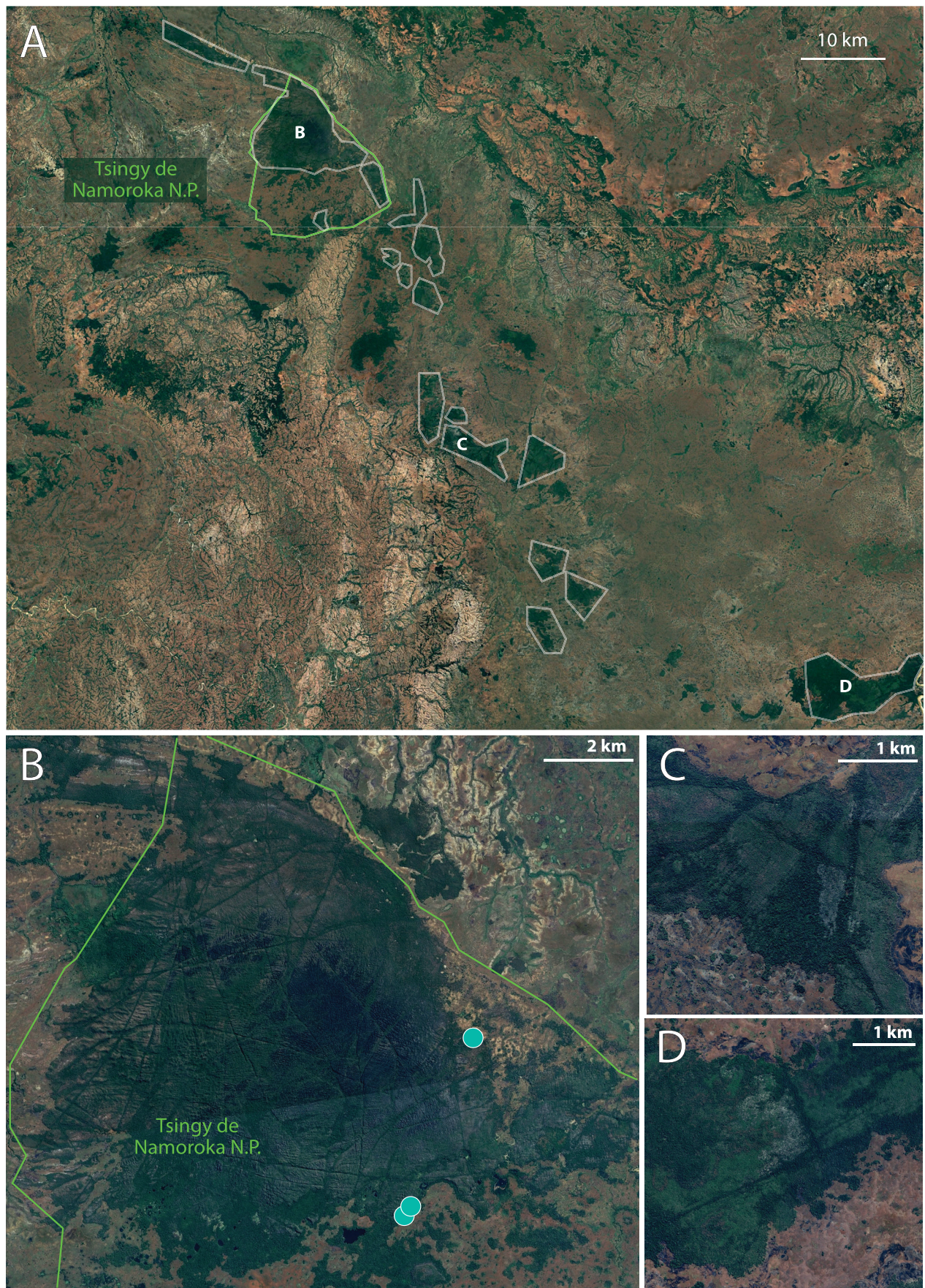


**Figure 6.** Satellite views of the Tsingy de Namoroka. **A** Namoroka National Park and surrounding areas. **B** Details of the main karstic area. **C, D** Details of areas here interpreted as vestigial karstic fragments located outside of the national park. Karstic fragments (i.e., showing the typical network of canyons/fissures arranged perpendicular to each other and filled with vegetation) are delimited in white, while the perimeter of the national park is delimited in green. Turquoise dots correspond to the known localities of *M. minotaurus* sp. nov. Satellite imagery from Airbus, via Google Earth.



is present in peripheral karstic isolates too (cf. Fig. 6). The possibility of a broader distribution within the region for this species remains however plausible and cannot be dismissed in the absence of additional data. Although the Namoroka massif is well preserved and currently shows no significant signs of anthropogenic disturbance, the new species' habitat is likely highly fragmented. Pending further information to confirm this species' range, population status, and potential threats, we recommended assigning the species the status VU (Vulnerable) based on the criteria D2 of the IUCN Standards and Petitions Committee (2024).

### *Madascincus irery* sp. nov.

<https://zoobank.org/C416E285-B102-46BD-B085-7B89ED840C0E>

Figures 7–12

**Holotype.** MADAGASCAR – **Diana Region** • unsexed specimen; Nosy Be, Lokobe National Park; 13°24'29"S, 48°18'31"E; ca. 210 m a.s.l.; 28 Apr. 2019, ca. 12:00 a.m.; M.D. Scherz, F. Glaw, A. Razafimanantsoa and J.H. Razafindralaibe leg.; ZSM 135/2019 (FGZC 5612).

**Paratype.** MADAGASCAR – **Diana Region** • 1 unsexed specimen; Nosy Be, Lokobe National Park; 13°24'31"S, 48°20'8"E; ca. 90 m a.s.l.; 18 Feb. 2015; "Frontier Madagascar" team leg.; ZSM 86/2015.

**Diagnosis.** *Madascincus irery* sp. nov. differs from all other species in the genus *Madascincus* (except those of the *nanus* group) by a lower number of ventral scales (55, versus 56 to 88), a short and pointed snout with visibly enlarged eyes and a dark and uniform coloration (versus lighter coloration, most often with dark lateral stripes variable in contrast and length). Additionally, it differs from the species of the *nanus* group by a higher number of scales around midbody (24, versus 18 to 20), and more elongated digits, with both a higher number of subdigital lamellae under the fourth finger (8, versus 3 to 5) and the fourth toe (12 to 15, versus 5 to 8). It differs from the species of the *polleni* group (its sister clade, formed by *M. polleni*, *M. arenicola*, *M. stumpffi* and *M. miafina*) by a distinctly lower number of ventral scales (55, versus 65 to 88) and of paravertebral scales (53 to 56, versus 65 to 88), a smaller size (33.8 to 39.9 mm, versus 54.9 to 89.6 mm), an hourglass-shaped frontal, i.e., constricted by the first pair of supraocular (versus always bell-shaped in all species except in *M. stumpffi*, where this state of character is variable), and a lower number of subdigital lamellae under the fourth toe (12 to 15, versus 15 to 23).

**Description of the holotype.** (Figs 10, 11) Presumably adult specimen, in an overall good state of preservation, with exception of the right hindlimb, which has been cut off as tissue sample, and a longitudinal row of approximately 20 scales ripped out on the left side of the

body. A rather small *Madascincus* species with relatively large eyes and short and pointed snout. SVL (33.8 mm) 7 times head length (5.9 mm), almost as long as tail (41.0 mm, apparently entire and not regenerated). Limbs very short: SVL 7.1 times forelimb length (5.5 mm) and 4.3 times hind limb length (8.9 mm). Snout short and rounded in lateral aspect and dorsal aspect. Rostral wider than high/long, contacting first supralabial scales, nasals, and supranasal scales. Paired supranasal scales in median contact, contacting loreals and postnasals. Frontonasal roughly triangular, wider than long, contacting loreals, first supraciliaries and first suprocular scales. Prefrontal scales absent. Frontal longer than wide, wider posteriorly, in contact with frontonasal, supraoculars, parietals and interparietal. Four supraoculars, all of them in contact with frontal; the second and third pairs larger than the anteriormost and posteriormost pairs; the first pair weakly constricting frontal (frontal hourglass-shaped sensu Andreone and Greer 2002). Frontoparietals absent. Interparietal longer than wide, well separated from supraoculars; parietal eyespot present with parietal eye evident. Parietals contact posterior to interparietal. Enlarged nuchals absent. Nasals slightly larger than nostrils; contacting rostral, first supralabials, postnasals and supranasals. Postnasals present, separating supranasals from first supralabials, and nasals from loreals. Loreal single, slightly higher than long. Preocular trapezoidal, as longer as high, single. Presubocular roughly triangular, elongated, single. Seven supraciliaries on both sides, in continuous row; first and last pairs significantly larger than the intermediate ones; last pair projecting onto supraocular shelf. Two pretemporals. Two postsuboculars; upper contacting lower pretemporal; both contacting penultimate supralabial. Lower eyelid moveable, scaly; lower palpebrals small, longer than high, interdigitating with large polygonal scales of central eyelid. Contact between upper palpebrals and supraciliaries seemingly direct but flexible, i.e., palpebral cleft narrow. Primary temporal single. Two secondary temporals; upper contacting lower pretemporal anteriorly and overlapping lower secondary temporal ventrally. Six supralabials, with the fourth being the enlarged subocular, contacting scales of the lower eyelid. External ear opening small, higher than wide, without lobules. Mental wider than long, posterior margin convex. Postmental wider than long, contacting first two pairs of infralabials. Six infralabials. Three pairs of large chin scales, both members of first pair in contact, both members of second pair separated by a single median scale, and members of third pair separated by three scale rows. No scales extending between infralabials and large chin scales. Gulars similar in size and outline to ventrals. All scales, except head shields and scales on palms, soles, and digits, cycloid, smooth, and imbricate; 24 longitudinal scale rows at midbody; 53 paravertebrals, similar in size to adjacent scales; 55 ventrals. Inner preanals overlapped by outer. Both anterior and posterior limbs pentadactyl; fingers and toes clawed; relative length of toes in the following order: I<II<III<V<IV. Subdigital lamellae smooth, single, with eight under both fourth finger, 12 under left fourth toe.

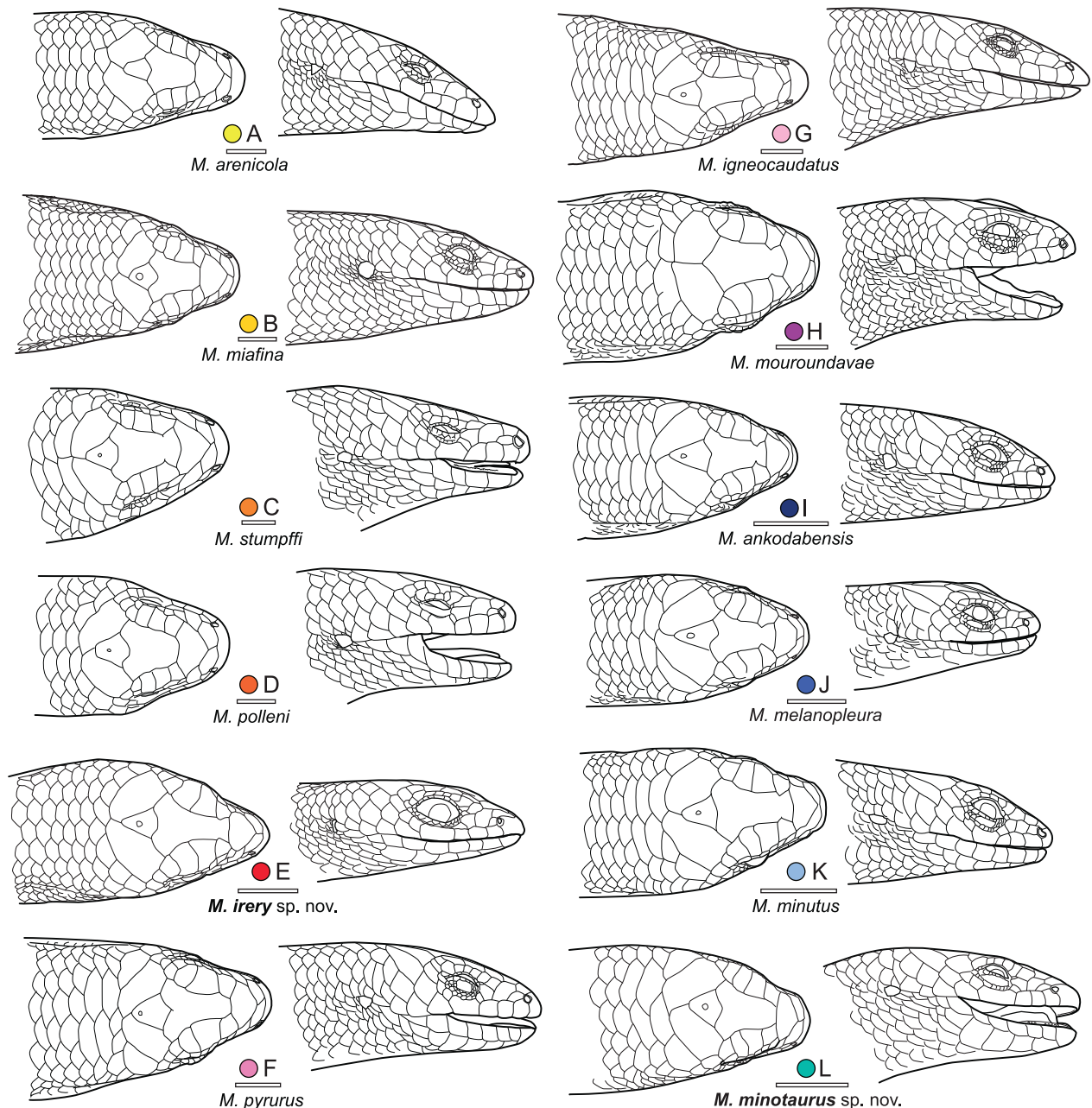


**Figure 7.** Drawings of the heads in dorsal and lateral views of most of the species of *Madascincus*. **A** *M. arenicola*, holotype ZSM 1565/2008, Baie des Sakalava. **B** *M. miafina*, holotype ZSM 1562/2008, Ankarana Special Reserve. **C** *M. stumpffi*, holotype SMF 16019, “Nossibé” (= Nosy Be). **D** *M. polleni*, holotype MNHN 1895.210, “Mouroundava” (= Morondava). **E** *M. irery* **sp. nov.**, holotype ZSM 135/2019, Nosy Be. **F** *Madascincus pyrurus*, holotype ZSM 520/2001, Mont Ibity. **G** *M. igneocaudatus*, ZSM 1600/2010, Anakao. **H** *M. mouroundavae*, ZSM 13/2005, Andasibe. **I** *M. ankodabensis*, ZSM 355/2006, Ranomafana. **J** *M. melanopleura*, ZSM 20/2005, Andasibe. **K** *M. minutus*, ZSM 400/2005, Nosy Mangabe. **L** *M. minotaurus* **sp. nov.**, holotype ZSM 116/2023, Namoroka. Dwarf species, namely *M. nanus* and *M. macrolepis*, not represented. Scale bars = 2 mm.

**Coloration of the holotype.** In preservative, specimen with a relatively uniform bronze coloration on the dorsal side from head to tail, slightly darker along two barely visible paravertebral lines, progressively fading on the flanks to become an immaculate light cream coloration on the ventral side. Palms and soles barely darker than the rest of the ventral side. In life, the coloration pattern was relatively similar to that in preservative, with however a slightly brighter and warmer overall aspect. The scales in life were iridescent (Fig. 10).

**Variation.** The paratype ZSM 0086/2015 is generally very similar to the holotype (Fig. 11). It has the following traits: SVL 39.9 mm, width at midbody 5.3 mm, tail length 52 mm, hindlimb 10.5 and 9.5 mm (right and left, respectively), 13 and 15 subdigital lamellae under the fourth toes, 55 ventrals, 56 dorsals, 24 scales around midbody.

**Etymology.** The specific epithet *irery*, invariable noun in apposition, is derived from the Malagasy language, and





**Figure 8.** Plate showing photographs in life of some of the recognized species of *Madascincus* (not to scale).

means “alone” or “solitary”. It refers both to the assumption that this species seems to be isolated on the small island of Nosy Be and the fact that it represents a distinct long phylogenetic branch.

**Distribution.** Only known from Lokobe National Park (east and west, and therefore likely widespread across the park) on Nosy Be (Fig. 12). Surveys on the adjacent

island of Nosy Komba failed to find this species (Hyde Roberts and Daly 2014; Blumgart et al. 2017).

**Ecology.** In 2019, the holotype of *M. irery* **sp. nov.** was collected active around noon on 28 April, on a boulder field next to a small stream on the Circuit Mitsinjo within Lokobe National Park. The microhabitat was characterized by large boulders covered in moss and liver-



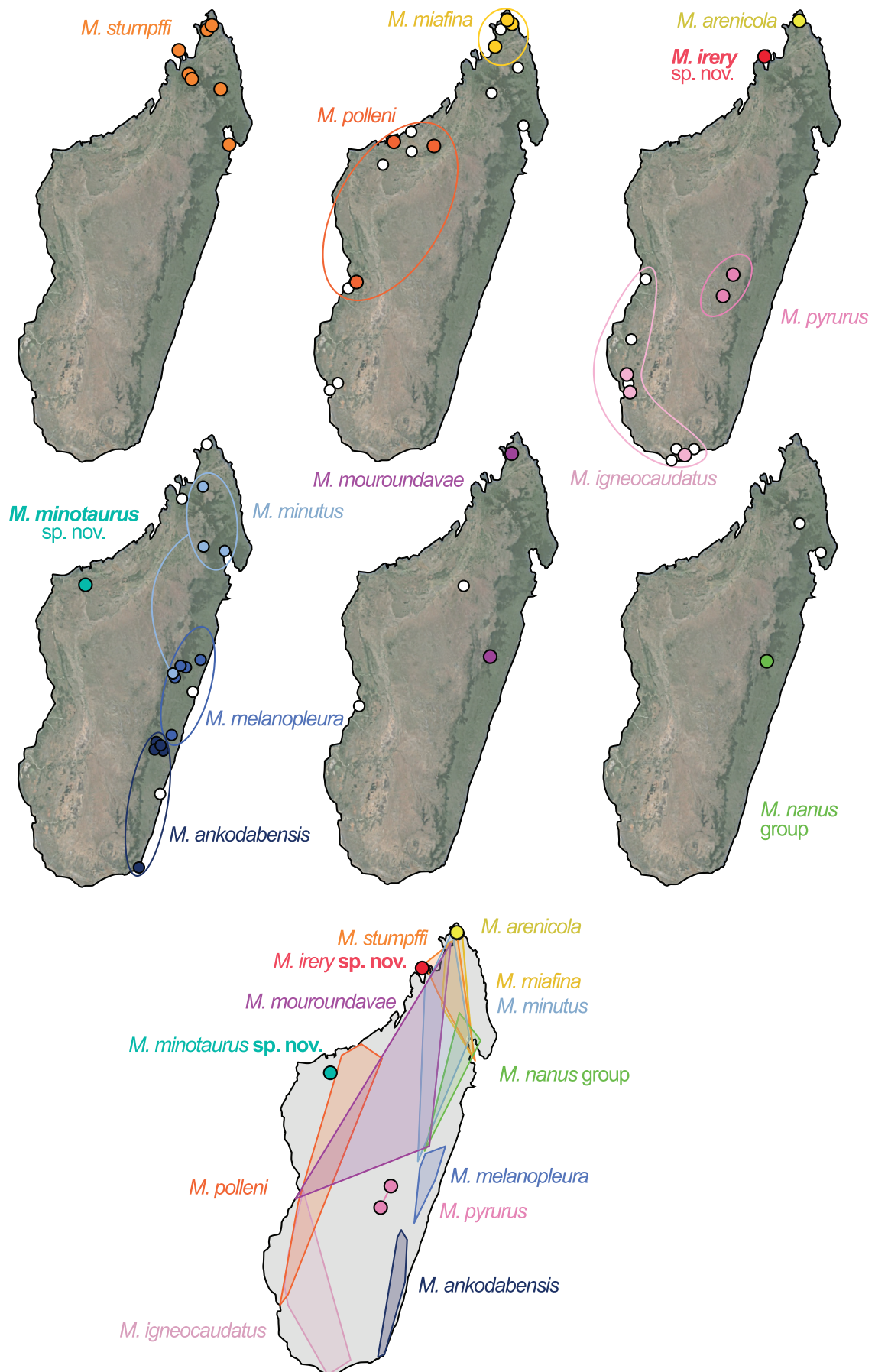


**Figure 9.** Schematic maps for Madagascar showing known distribution for *Madascincus* species. For reasons of readability, the different species are shown on six separate maps. Colored dots represent localities confirmed by DNA sequences, whereas white dots represent localities of specimens only identified by morphology (more details in Miralles et al. 2016). The supplementary map located at the bottom of the figure, employs minimum convex polygons to compare the distribution ranges of all species.

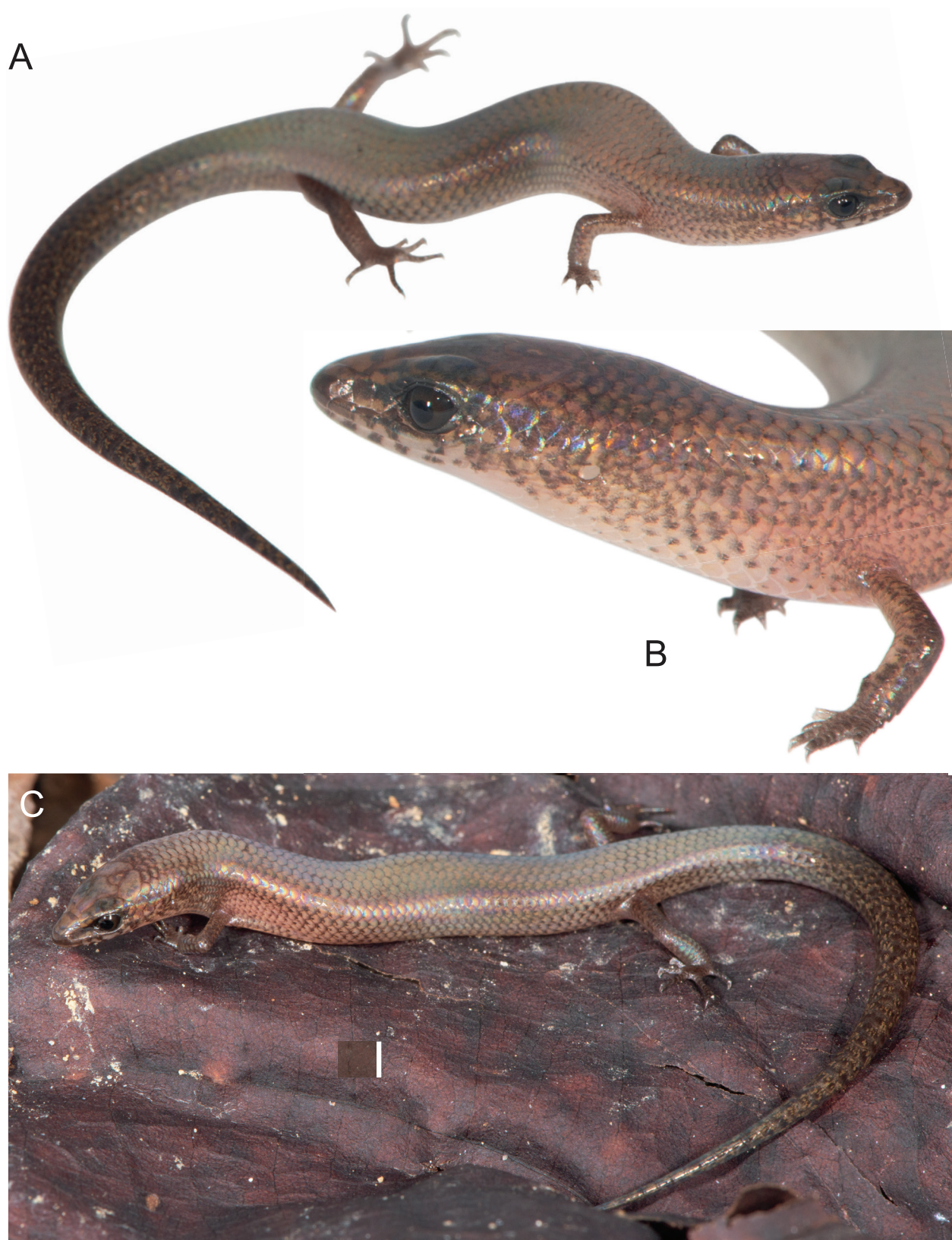


**Figure 10.** Alive picture of *Madascincus irery* sp. nov. A, B, C Holotype ZSM 135/2019, from Lokobe National Park, Nosy Be. Photographs by MDS.

worts (Fig. 12C). This kind of habitat occurs in several locations within Lokobe, which is comprised mostly of lowland moist evergreen forest, but our brief survey did not find the species elsewhere. Far more comprehensive

fieldwork is needed to establish the spread of the species within the park, and surveys in other forest fragments on the island should be carried out to establish whether it occurs outside the park.



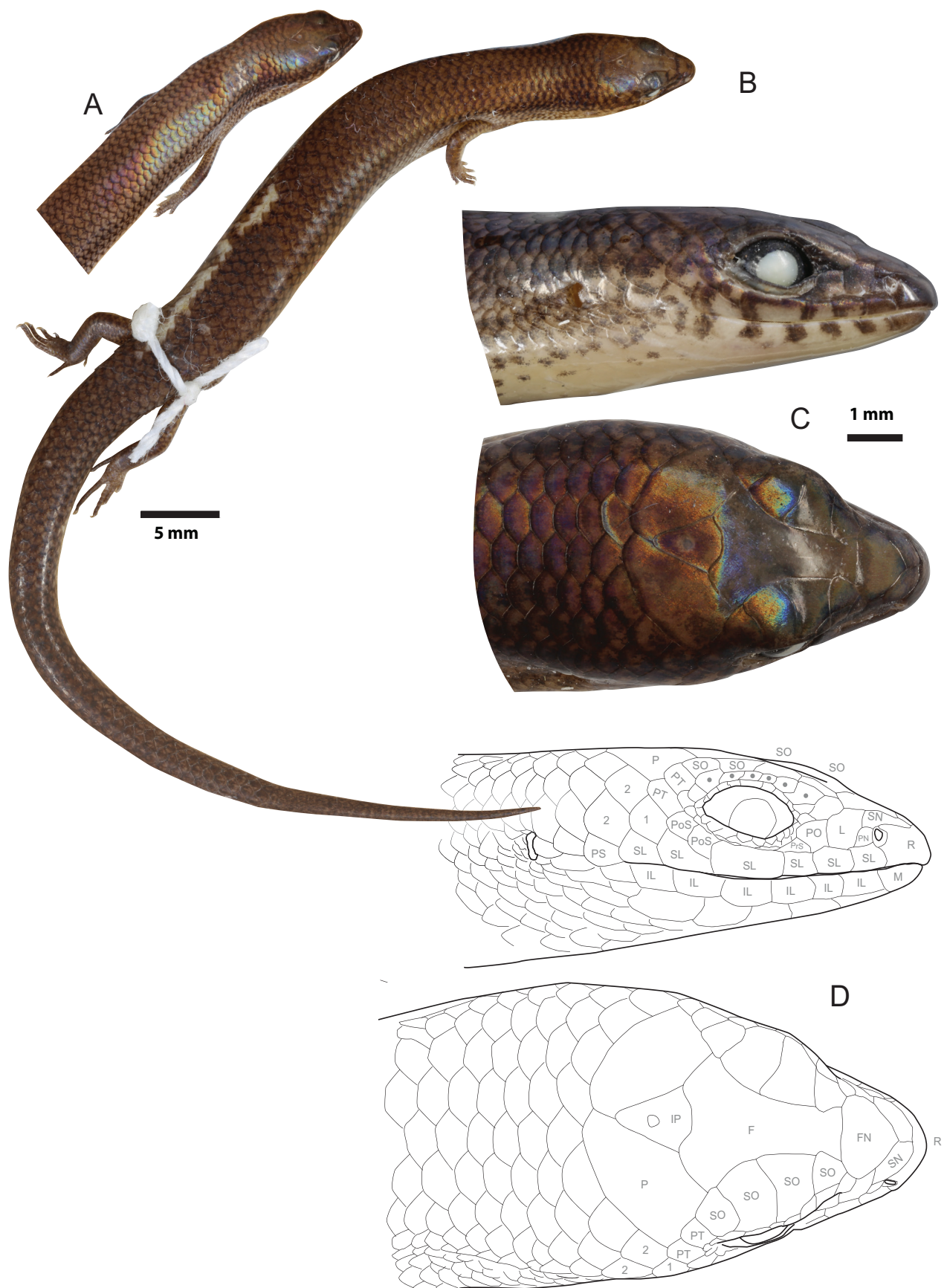


**Figure 11.** Preserved specimens of *Madascincus irery* sp. nov. **A** Anterior body of the paratype, ZSM 86/2015 in dorsal view. **B** dorsal view of the entire body, **C** lateral and dorsal view of the head, **D** drawing of head in lateral and dorsal views of holotype ZSM 135/2019 from Lokobe National Park. Abbreviations used in the drawings are explained in the Materials and Methods section.



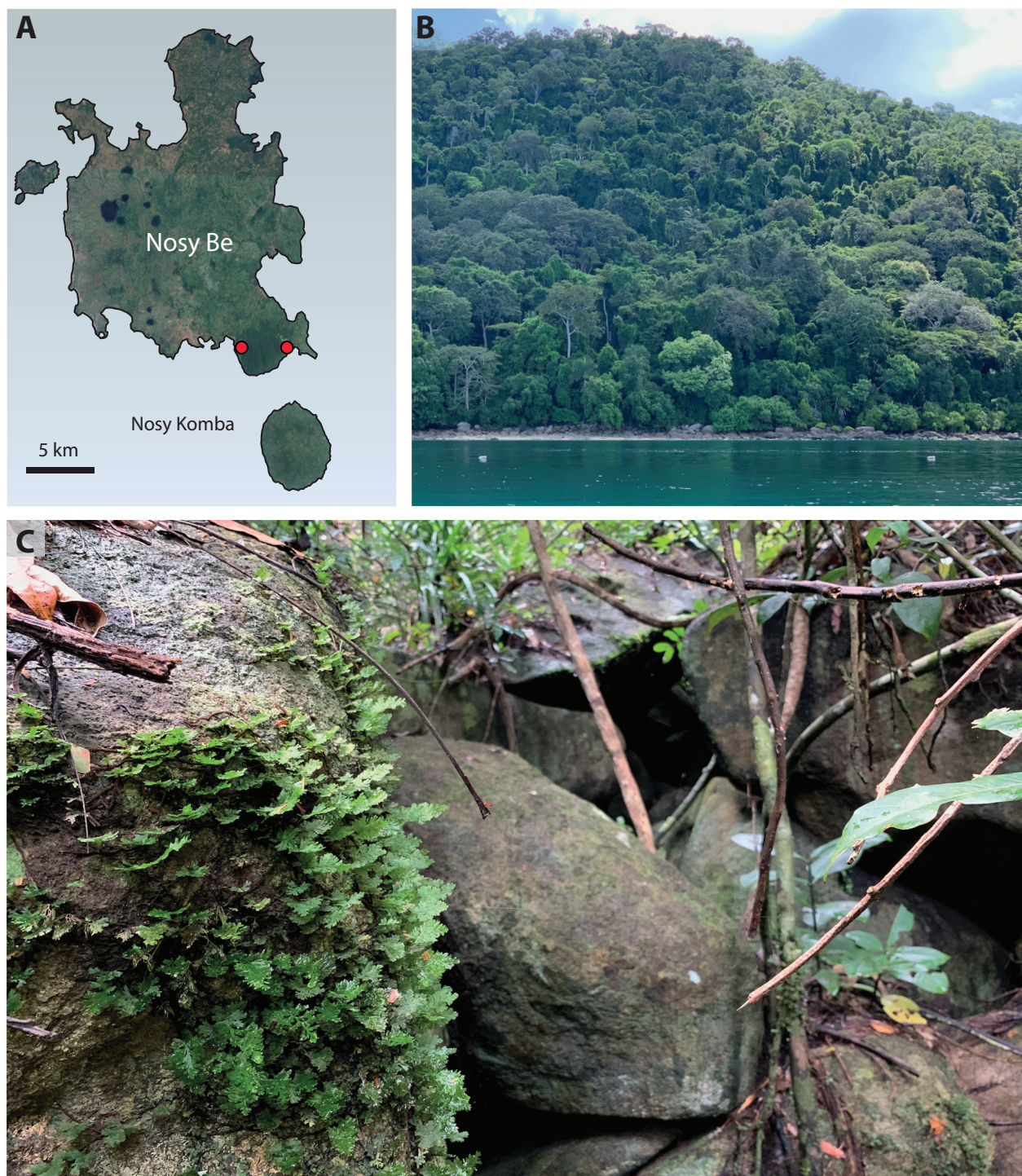


**Figure 12.** **A** Map indicating known localities of *Madascincus irery* sp. nov. on Nosy Be (red dots). **B** Forest at the Lokobe National Park. **C** Detail of the habitat where the holotype of *Madascincus irery* sp. nov. was collected.

**Conservation status.** Considering that *Madascincus irery* sp. nov. is likely widely distributed across the Lokobe reserve, its EOO might be at least of 7.4 km<sup>2</sup> (Andreone et al. 2003). The possibility of a broader distribution within Nosy Be island for this species remains however plausible and cannot be dismissed in the absence of additional data. The Lokobe area exhibits a largely intact forest cover, and direct anthropogenic pressures in its central protected areas remain limited. However, the distribution range of *Madascincus irery* sp. nov. is extremely restrict-

ed (possibly less than 10 km<sup>2</sup>), warranting particular attention and regular monitoring to assess its global risk of extinction. Pending further information to confirm this species' range, population status, and potential threats, we recommend to assign the species the status VU (Vulnerable) according to the criteria D2 of the IUCN Standards and Petitions Committee (2024).



## Discussion

### Integrative species delimitation

The two new species described here are known from a very limited sampling (one sequenced voucher specimen for *M. minotaurus* and two for *M. irery*). Nevertheless, their recognition as distinct species is robustly supported by independent lines of evidence. Each species represents a highly divergent and likely ancient lineage within the genus, as supported by the substantial branch lengths obtained independently in the mitochondrial and in the nuclear phylogenetic trees. Accordingly, the 16S uncorrected p-distances calculated between *M. irery* **sp. nov.** and the species in its sister clade (7.4–9.3%), and those between *M. minotaurus* **sp. nov.** and its sister clade (9.0–10.9%) correspond to those already obtained between recognized species in the genus (mean = 8.5%, min–max = 2.8–12.5%,  $N = 55$  species pair comparisons), and are two to three times higher than intraspecific distances which, for the same genus and the same genetic marker never exceed 3.1% ( $N = 11$  species, data from Miralles et al. 2016). Both species also exhibit several morphological characteristics that unambiguously differentiate them from all other species known in the genus in general, and from their closest relatives (sister clades) in particular.

### Biogeography

The completion of a full inventory of life on Earth is inherently challenging, as it is impossible to anticipate with certainty where undescribed species remain to be found. Taxonomic discoveries, however, do not rely solely on chance. Exploration targeting remote, isolated and understudied regions that possess distinct ecological characteristics in contrast to those prevailing in the surrounding areas holds the potential for the discovery of ancient or relict lineages. The more ancient and ecologically isolated these regions are, the more likely they may have served as refugia where evolutionary processes followed unique and divergent trajectories. This assumption is exemplified by the present study, which highlights the existence of two new species found opportunistically, each representing deeply divergent phylogenetic lineages within the genus *Madascincus* and appearing to have highly restricted geographic distributions. As such, they provide novel insights into the biogeographic history of the genus:

*Madascincus irery* **sp. nov.** might be endemic to Nosy Be (but should also be sought on adjacent islands and in adjacent areas of the Sambirano region on mainland Madagascar), while its sister group, the *polleni* clade, is primarily confined to the northern part of mainland Madagascar (except for *M. polleni*, which is found slightly further south, in the North West, Fig. 9). Although some important early taxonomic works on the Malagasy herpetofauna were based on material sent to Europe from Nosy Be (Boettger 1880, 1881; Peters 1880; Vaillant 1885), scientific exploration of the island—which today

**Table 1.** Comparison of the most relevant morphological characters in *Madascincus* species. Ranges are given for meristic and mensural characters, followed by the mean  $\pm$  the standard deviation, with sample size in parentheses. For bilateral characters, the sample size was noted as the number of sides rather than specimens. Data from Andreone and Greer (2002), Glaw and Vences (2007), Miralles et al. (2011a, 2016), Miralles and Vences (2013), Porcel et al. (2021). Spec. – spectacled; vivi. – viviparous; ovi. – oviparous.

		igneocaudatus	pyrrhus	minutus	melano-pleura	ankodabensis	mou-roundavae	nanus group	arenicola	miqfina	polleni	stumpffi	minotaurus sp. nov.	irery sp. nov.
N lamellae under 4 <sup>th</sup> finger	min-max: mean $\pm$ SD: n sides:	8–11 9.0 $\pm$ 0.9 (50)	8–11 9.1 $\pm$ 0.9 (14)	5–7 6.0 $\pm$ 0.8 (13)	5–8 7.0 $\pm$ 0.6 (40)	5–8 6.3 $\pm$ 1.0 (9)	8–11 9.8 $\pm$ 0.7 (16)	3–5 3.9 $\pm$ 0.6 (8)	6–7 6.4 $\pm$ 0.5 (11)	7–8 7.6 $\pm$ 0.5 (22)	6–9 7.5 $\pm$ 0.7 (26)	6–9 7.3 $\pm$ 0.8 (27)	7 — (1)	8 8.0 $\pm$ 0.0 (3)
N lamellae under 4 <sup>th</sup> toe	min-max: mean $\pm$ SD: n sides:	15–22 18.1 $\pm$ 1.4 (54)	15–18 16.4 $\pm$ 1.3 (13)	9–13 11.3 $\pm$ 1.5 (10)	12–16 14.1 $\pm$ 1.2 (52)	12–15 13.8 $\pm$ 1.1 (12)	16–20 17.5 $\pm$ 1.2 (15)	5–8 6.8 $\pm$ 1.3 (9)	16–19 17.5 $\pm$ 0.8 (13)	18–23 20.6 $\pm$ 1.3 (20)	16–22 18.5 $\pm$ 1.5 (22)	15–20 17.9 $\pm$ 1.2 (28)	15 — (1)	12–15 13.3 $\pm$ 1.5 (3)
N ventral scale rows	min-max: mean $\pm$ SD: n:	68–83 76.7 $\pm$ 4.4 (21)	73–78 75.7 $\pm$ 1.8 (7)	55–63 58.3 $\pm$ 3.0 (7)	56–61 58.8 $\pm$ 1.2 (27)	59–63 60.2 $\pm$ 1.5 (6)	63–66 64.3 $\pm$ 1.0 (8)	52–60 57.6 $\pm$ 3.3 (5)	75–80 77.9 $\pm$ 1.6 (7)	65–73 68.7 $\pm$ 2.1 (14)	74–78 75.8 $\pm$ 1.2 (12)	70–88 81.3 $\pm$ 4.0 (16)	68 — (1)	55 55.0 $\pm$ 0.0 (2)
N paravertebral scale rows	min-max: mean $\pm$ SD: n:	69–80 74.7 $\pm$ 3.0 (26)	71–79 74.6 $\pm$ 3.7 (7)	57–65 59.7 $\pm$ 3.4 (7)	51–62 55.9 $\pm$ 2.9 (28)	52–62 57.7 $\pm$ 3.1 (7)	60–65 62.6 $\pm$ 2.1 (8)	50–57 53.6 $\pm$ 2.5 (5)	74–81 79.0 $\pm$ 2.3 (7)	65–79 68.7 $\pm$ 3.3 (14)	71–81 77.9 $\pm$ 2.6 (13)	76–88 82.7 $\pm$ 3.2 (15)	69 — (1)	53–56 54.5 $\pm$ 2.12 (2)

		<i>ignecoccus</i> <i>datus</i>	<i>pyrus</i>	<i>minutus</i>	<i>melano-</i> <i>pleura</i>	<i>ankoda-</i> <i>bensis</i>	<i>mou-</i> <i>roundavae</i>	<i>nanus</i> group	<i>arenicola</i>	<i>miatna</i>	<i>polleni</i>	<i>stumpffii</i>	<i>minotaurus</i> sp. nov.	<i>ivery</i> sp. nov.
	min-max; mean ± SD; n:	24–26 24.2 ± 0.6 (28)	22–24 23.3 ± 1.0 (7)	22–26 24.0 ± 1.2 (7)	24–26 24.1 ± 0.4 (27)	22–26 23.7 ± 1.5 (6)	28–30 29.0 ± 4.2 (8)	18–20 19.6 ± 0.9 (5)	26 26.0 ± 0 (7)	24–26 24.1 ± 0.5 (14)	24–26 25.4 ± 0.9 (13)	30–32 31.6 ± 0.8 (16)	20 — (1)	24 24.0 ± 0.0 (2)
Enlarged nuchal scales	absent: one row: two rows: three rows: four rows: n sides:	— — 23.2% 71.4% 5.4% (56)	— — 21.4% 78.6% — (14)	— — 28.6% 57.1% 14.3% (14)	— 2% 48% — (58)	— 7.1% 35.8% 57.1% — (14)	— 100% — — (16)	— 40.0% 20.0% 40.0% — (10)	42.9% 57.1% — — (14)	92.3% 7.7% — — (26)	56.3% 37.5% 6.2% — (22)	81.3% 18.7% — — (32)	— — 100% — (2)	100% — — — (4)
Postnasal	present: absent: n sides:	100% — (56)	100% — (14)	100% — (14)	100% — (58)	100% — (14)	100% — (16)	100% — (10)	— 100% (14)	89.3% 10.7% (28)	100% — (26)	94.4% 5.6% (36)	100% — (2)	100% — (4)
Frontal and interpa- rietal	fused: separated: n:	— 100% (28)	— 100% (14)	— 100% (7)	— 100% (28)	— 100% (7)	87.5% 12.5% (8)	— 100% (10)	— 100% (7)	— 100% (14)	— 100% (13)	— 100% (16)	— 100% (1)	— 100% (1)
Frontal	bell-shaped: hour-glass shaped: n:	100% — — (23)	100% — — (12)	— 100% — (14)	— 100% — (29)	— 100% — (14)	— 100% — (8)	— 100% — (10)	100% — — (7)	100% — — (14)	100% — — (13)	47.2% 52.8% — (18)	100% — — (1)	— 100% — (2)
Snout-vent length (mm)	max: mean ± SD: n:	73.0 56.3 ± 11.6 (9)	54.2 52.3 ± 2.1 (4)	47.4 42.0 ± 5.1 (7)	53.5 49.5 ± 2.5 (21)	50.5 48.0 ± 2.4 (5)	68.5 60.1 ± 9.6 (7)	33.6 27.8 ± 8.2 (6)	81.7 72.3 ± 6.1 (7)	61 54.9 ± 3.1 (14)	75 66.0 ± 7.1 (13)	114.0 89.6 ± 10.8 (14)	39.9 — (1)	39.9 36.9 ± 4.1 (2)
Supraciliaries	five: six: seven: eight: n sides:	— 98.2% 1.8% — (56)	7.1% 92.9% — — (14)	7.1% 57.1% 35.8% (14)	— 8.6% 79.3% 12.7% (58)	— 35.7% 50.0% 14.3% (14)	— 93.8% 6.2% — (16)	— 66.6% 33.3% — (6)	— 92.9% 7.1% — (14)	— 100% — — (2)	— 87.5% 12.5% — (8)	n/a — — — (2)	— 100% — — (2)	— 100% — — (2)
Subocular	third SL: fourth SL: n sides:	1.8% 98.2% (56)	— 100% (14)	— 100% (14)	— 100% (58)	7.1% 92.9% (14)	— 100% (24)	100% — (10)	— 100% (14)	3.6% 96.4% (28)	— 100% (24)	— 100% (32)	— 100% (2)	— 100% (4)
Lower eyelid window		spec.	spec.	spec.	spec.	spec.	scaly	scaly	scaly	scaly	scaly	scaly	spec.	scaly
Reproduction*		vivi.	ovi.	?	?	?	ovi.	ovi.	?	?	?	?	ovi?	?
Elevational range		≤ 500 m	≥ 1500 m	≤ 1000 m	≤ 1000 m	≤ 1000 m	≤ 1000	500–1500 m	≤ 500 m	≤ 500 m	≤ 500 m	≤ 500 m	≤ 500 m	≤ 500 m

is a hotspot for tourism with an international airport—has been limited (Andreone et al. 2003). This new *Madascincus* species represents the second to be reported from Nosy Be, alongside *Madascincus stumpffi*, which appears to be more opportunistic, with a broad distribution across multiple localities throughout this island (Andreone et al. 2003; iNaturalist). These results support the hypothesis according to which the *polleni* clade most likely originated and diversified in northern Madagascar.

*Madascincus minotaurus* **sp. nov.** is only known from the Tsingy de Namoroka, a karstic system located in the dry West of Madagascar. Its sister clade (the *melanopleura* group) is contrastingly distributed across the entire humid eastern part of the island (and likely has an origin in the North, Fig. 9). Interestingly, a similar biogeographic pattern can be found in the Velvet geckos (genus *Blaesodactylus* Boettger, 1893), with *B. victori* Ineich, Glaw & Vences, 2016, also endemic to Namoroka, which has been recovered as sister group of *B. microtuberculatus* Jono, Bauer, Brennan & Mori, 2015, a species only found in the North of the island (Vences et al. 2025). Such biogeographical affinities between Namoroka and the North suggest these two regions might have been connected in the past, during a period when the climate was more humid. The Tsingy de Namoroka massif appears to offer a distinct microclimate—cooler and more humid than the surrounding Mahajanga region, which is otherwise characterized by a prolonged dry season. This unique set of conditions may have served as a climatic refuge for the local fauna. Likely contributing to this microclimate, the area indeed experiences substantial flooding during the rainy season and benefits year-round from a natural cooling effect generated by an extensive network of caves, where water reservoirs persist even through the dry season. (A.M. pers. obs., Fig. 5E; see also Vences et al. 2025 for more details on the Tsingy de Namoroka habitat).

The Tsingy of Namoroka represents a region of high interest to the scientific community due to the important number of apparently micro-endemic species hosted by these karst formations. This remarkable level of endemism appears to affect a wide range of taxonomic groups, including plants (Wilkin et al. 2002; Gautier et al. 2022), insects (Paulian and Grjebine 1953; Synave 1953; Risbec 1956; Chlond et al. 2018; Faille and Lecoq 2018; Guilbert 2020), arachnids (Lourenço and Goodman 2004; Wood 2008; Lourenço and Wilmé 2019) and squamates (Ineich et al. 2016; Rakotoarison et al. 2025; Vences et al. 2025). Satellite imagery analysis indicates that the Namoroka karst system extends well beyond the current boundaries of the national park (Fig. 6). In the northwestern direction, a wide continuous karstified band stretches over approximately 17 km, suggesting significant continuity (Fig. 6A). To the southeast, several isolated karst features, each spanning from two to ten kilometers long, are scattered over a distance of roughly 100 km, following a roughly linear alignment reaching the Mahamay river. Although the southernmost formations appear to be more heavily eroded, the presence of densely vegetated canyons intersecting at near-perpendicular angles is a distinctive morphological feature, closely resembling the

structure observed in the main Namoroka karst area (Fig. 6C, D). Given that these distinct karst outcrops were likely connected in the past, it is plausible that *Madascincus minotaurus* **sp. nov.**, along with other Namoroka endemic species, might also persist in these areas. Due to their relative inaccessibility, these isolated areas remain poorly explored, and comprehensive field surveys are warranted to evaluate their local biodiversity and to identify potential conservation priorities associated with these remote environments.

## Conclusion

This paper increases the number of described species in the genus *Madascincus* from 12 to 14. However, the species inventory for this genus is not yet complete, as suggested by the identification of at least three credible, as-yet-undescribed candidate species within the genus in previous studies: *Madascincus* sp. “baeus” (cf. Glaw and Vences 2007) and *Madascincus* sp. “Betampona” (Belluardo et al. 2023; work in preparation), two candidate species belonging to the *M. nanus* group, as well as *Madascincus* sp. “vitreus”, a candidate species identified in the Morondava region, and likely belonging to the *M. igneocaudatus* group (Glaw and Vences 2007). Furthermore, *M. minutus*, located at the northern tip of the island, might represent a complex of several morphologically cryptic species, given the considerable genetic diversity observed within this taxon (Miralles and Vences 2013; Miralles et al. 2016). Finally, as illustrated by the present study, it is also possible that species yet to be collected remain undiscovered in various parts of the island, even those heavily visited by tourists and local researchers.

## Acknowledgments

We are grateful to Ivan Ineich, Gabriele Keunecke, Ny Ando Tsiky Rahagalala, Angeluc Razafimanantsoa, Mathilde Aladini, Jérôme Courtois, Stéphane Grosjean, Didier Geffard-Kuriyama, Jary H. Razafindralaibe, and Fanomezana M. Ratsoavina for advice and/or help with logistics, field work or laboratory work. Fieldwork was carried out in the framework of a collaboration accord between the Technische Universität Braunschweig, the Université d’Antananarivo, and the Ministry of the Environment and of the Sustainable Development. Many thanks to Ishan Agarwal, Uwe Fritz, Daniel Jablonski and Jörn Köhler, who provided valuable comments that helped to improve the manuscript. AM and MV acknowledges support from the Deutsche Forschungsgemeinschaft (grant MI 2748/1-1) and the Agence Nationale de la Recherche (ANR-24-CPJ1-0129-01). Thanks are due to the Malagasy authorities, in particular to the Ministry of the Environment and of the Sustainable Development and Madagascar National Parks, for research, collection and export permits (research permit 315/23/MEDD/SG/DGGE/DAPRNE/SCBE.Re; MNP access permit to Tsingy de Namoroka National Park 158/2023). Authors are also grateful to the Atelier Iconographie Scientifique, UAR 2700 2AD, BAOBAB facilities supported by DIM-MAP Île-de-France, CNRS and MNHN.



## References

- Andreone F, Glaw F, Nussbaum RA, Raxworthy CJ, Vences M, Randrianirina JE (2003) The amphibians and reptiles of Nosy Be (NW Madagascar) and nearby islands: A case study of diversity and conservation of an insular fauna. *Journal of Natural History* 37: 2119–2149. <https://doi.org/10.1080/00222930210130357>
- Andreone F, Greer AE (2002) Malagasy scincid lizards: Descriptions of nine new species, with notes on the morphology, reproduction and taxonomy of some previously described species (Reptilia, Squamata: Scincidae). *Journal of Zoology* 258: 139–181. <https://doi.org/10.1017/S0952836902001280>
- Belluardo F, Muñoz-Pajares AJ, Miralles A, Silvestro D, Cocca W, Ratsoavina FM, Villa A, Hyde Roberts S, Mezzasalma M, Zizka A, Antonelli A, Crottini A (2023) Slow and steady wins the race: Diversification rate is independent from body size and lifestyle in Malagasy skinks (Squamata: Scincidae: Scincinae). *Molecular Phylogenetics and Evolution* 178: 107635. <https://doi.org/10.1016/j.ympev.2022.107635>
- Blumgart D, Dolhem J, Raxworthy CJ (2017) Herpetological diversity across intact and modified habitats of Nosy Komba Island, Madagascar. *Journal of Natural History* 51: 625–642. <https://doi.org/10.1080/00222933.2017.1287312>
- Boettger O (1880) Diagnoses reptilium et batrachiorum novorum a Carolo Ebenau in insula Nossi-Bé madagascariensi lectorum. *Zoologischer Anzeiger* 3: 279–283.
- Boettger O (1881) Diagnoses reptilium et batrachiorum novorum ab ill. Antonio Stumpff in insula Nossi-Bé Madagascariensi lectorum. *Zoologischer Anzeiger* 4: 358–362.
- Boumans L, Vieites DR, Glaw F, Vences M (2007) Geographical patterns of deep mitochondrial differentiation in widespread Malagasy reptiles. *Molecular Phylogenetics and Evolution* 45: 822–839. <https://doi.org/10.1016/j.ympev.2007.05.028>
- Brown JL, Sillero N, Glaw F, Bora P, Vieites DR, Vences M (2016) Spatial biodiversity patterns of Madagascar's amphibians and reptiles. *PLoS One* 11: e0144076. <https://doi.org/10.1371/journal.pone.0144076>
- Chlond D, Guilbert E, Faille A, Bañar P, Davranoglou L-R (2018) A remarkable new species of cavernicolous Collartiini from Madagascar (Hemiptera: Heteroptera: Reduviidae). *Zootaxa* 4425: 372–384. <https://doi.org/10.11646/zootaxa.4425.2.11>
- Crottini A, Madsen O, Poux C, Strauß A, Vieites DR, Vences M (2012) Vertebrate time-tree elucidates the biogeographic pattern of a major biotic change around the K–T boundary in Madagascar. *Proceedings of the National Academy of Sciences of the United States of America* 109: 5358–5363. <https://doi.org/10.1073/pnas.1112487109>
- Erens J, Miralles A, Glaw F, Chatrou LW, Vences M (2017) Extended molecular phylogenetics and revised systematics of Malagasy scincine lizards. *Molecular Phylogenetics and Evolution* 107: 466–472. <https://doi.org/10.1016/j.ympev.2016.12.008>
- Faille A, Lecoq JC (2018) *Oedichirus spelaesus* n. sp., the first cave dwelling beetle from Madagascar (Coleoptera: Staphylinidae: Paederinae). *Journal of Cave and Karst Studies* 80: 13–18. <https://doi.org/10.4311/2017LSC0112R2>
- Gautier L, Boluda CG, Randrianaivo R, Naciri Y (2022) Two further new species in the highly-diverse Malagasy endemic genus *Capurodendron* (Sapotaceae). *Candollea* 77: 119–126. <https://doi.org/10.15553/c2022v771a9>
- Glaw F, Vences M (2007) A Field Guide to the Amphibians and Reptiles of Madagascar. Third Edition. Vences & Glaw Verlag, Cologne, 496 pp.
- Guilbert E (2020) New species of Tingidae (Insecta: Heteroptera) from Madagascar. *Zootaxa* 4759: 391–404. <https://doi.org/10.11646/zootaxa.4759.3.5>
- Hyde Roberts S, Daly C (2014) A rapid herpetofaunal assessment of Nosy Komba Island, northwestern Madagascar, with new locality records for seventeen species. *Salamandra* 50: 18–26.
- Ineich I, Glaw F, Vences M (2016) A new species of *Blaesodactylus* (Squamata: Gekkonidae) from Tsingy limestone outcrops in Namoroka National Park, north-western Madagascar. *Zootaxa* 4109: 523–541. <https://doi.org/10.11646/zootaxa.4109.5.2>
- IUCN Standards and Petitions Committee (2024) Guidelines for Using the IUCN Red List Categories and Criteria. Version 16. Prepared by the Standards and Petitions Committee. <https://www.iucnredlist.org/resources/redlistguidelines> [accessed 1 October 2025]
- Lourenço WR, Goodman SM (2004) A new species of *Tityobuthus* (Pocock) from Namoroka in the Province of Mahajanga, Madagascar (Scorpiones, Buthidae). *Revista Ibérica Aracnología* 9: 19–22.
- Lourenço WR, Wilmé L (2019) Scorpions from the Parc National du Tsingy de Namoroka, Madagascar and description of a new species of *Opisthacanthus* Peters, 1861 (Scorpiones: Hormuridae). *Revista Ibérica de Aracnología* 34: 13–20.
- Miralles A (2006) A new species of *Mabuya* (Reptilia, Squamata, Scincidae) from the Caribbean island of San Andrés, with a new interpretation of nuchal scales: A character of taxonomic importance. *Herpetological Journal* 16: 1–7.
- Miralles A, Crottini A, Raselimanana AP (2022) Scincidae, skinks. Andronga, Matahotrandro. In: Benstead JP, Goodman SM (Eds) *The New Natural History of Madagascar*. Princeton University Press, Princeton, NJ, 1494–1502. <https://doi.org/10.2307/j.ctv2ks6tbb.215>
- Miralles A, Hipsley CA, Erens J, Gehara M, Rakotoarison A, Glaw F, Müller J, Vences M (2015) Distinct patterns of desynchronized limb regression in Malagasy scincine lizards (Squamata, Scincidae). *PLoS One* 10: e0126074. <https://doi.org/10.1371/journal.pone.0126074>
- Miralles A, Köhler J, Glaw F, Vences M (2011a) A molecular phylogeny of the *Madascincus polleti* species complex, with description of a new species of scincid lizard from the coastal dune area of northern Madagascar. *Zootaxa* 2876: 1–16. <https://doi.org/10.11646/zootaxa.2876.1.1>
- Miralles A, Köhler J, Glaw F, Vences M (2016) Species delimitation methods put into taxonomic practice: Two new *Madascincus* species formerly allocated to historical species names (Squamata: Scincidae). *Zoosystematics and Evolution* 92: 257–275. <https://doi.org/10.3897/zse.92.9945>
- Miralles A, Köhler J, Vieites DR, Glaw F, Vences M (2011b) Hypotheses on rostral shield evolution in fossorial lizards derived from the phylogenetic position of a new species of *Paracontias* (Squamata, Scincidae). *Organisms Diversity and Evolution* 11: 135–150. <https://doi.org/10.1007/s13127-011-0042-6>
- Miralles A, Raselimanana AP, Rakotomalala D, Vences M, Vieites DR (2011c) A new large and colorful skink of the genus *Amphiglossus* from Madagascar revealed by morphology and multilocus molecular study. *Zootaxa* 2918: 47–67. <https://doi.org/10.11646/zootaxa.2918.1.5>
- Miralles A, Schmidt R, Rakotoarison A, Delaunay A, Freiwald A, Rahagalala NA, Rakotomanga R, Razafimanafy D, Ratsoavina FM, Crottini A, Raselimanana AP, Glaw F, Vences M (2025) Integrative taxonomy of Madagascar's sand-swimming skinks (Scincidae: *Voeltzkowia*, *Grandidierina*) and preliminary evidence for an overlooked inland belt of white sand patches across the island's west.

- Zoological Journal of the Linnean Society 205: zlaf147. <https://doi.org/10.1093/zoolinnean/zlaf147>
- Miralles A, Vences M (2013) New metrics for comparison of taxonomies reveal striking discrepancies among species delimitation methods in *Madascincus* lizards. PLoS One 8: e68242. <https://doi.org/10.1371/journal.pone.0068242>
- Nylander JAA (2004) MrModeltest v2. Program distributed by the author. Evolutionary Biology Centre, Uppsala University, Uppsala. <https://github.com/nylander/MrModeltest2> [accessed 10 January 2025]
- Paulian R, Grjebine A (1953) Une campagne spéléologique dans la réserve naturelle de Namoroka. Naturaliste Malgache 5: 19–28.
- Peters W (1880) Über die von Hrn. J. M. Hildebrandt auf Nossi-Bé und Madagascar gesammelten Säugethiere und Amphibien. Monatsberichte der Königlich Preussischen Akademie der Wissenschaften zu Berlin 1880: 508–511.
- Porcel X, Dubos N, Rosa GM, Miralles A, Noël J, Lava H, Velo JH, Andreone F, Crottini A (2021) The kiwi of all skinks: An unusual egg size in a species of *Madascincus* (Scincidae: Scincinae) from eastern Madagascar. Herpetology Notes 14: 365–369.
- Rakotoarison A, Gippner S, Multzsch M, Miralles A, Razafimanafa D, Hasiniaina A, Glaw F, Vences M (2025) Molecular systematics of the enigmatic dwarf gecko *Lygodactylus ornatus* and description of a new species of the *L. verticillatus* group from the North West of Madagascar. Zootaxa 5621: 420–436. <https://doi.org/10.11646/zootaxa.5621.4.2>
- Risbec J (1956) Tormyidae et Agaonidae de Madagascar (Hym. Chalcidoidea). Annales de la Société Entomologique de France 124: 149–194.
- Ronquist F, Huelsenbeck JP (2003) MRBAYES 3: Bayesian phylogenetic inference under mixed models. Bioinformatics 19: 1572–1574. <https://doi.org/10.1093/bioinformatics/btg180>
- Schmitz A, Brandley MC, Mausfeld P, Vences M, Glaw F, Nussbaum RA, Reeder TW (2005) Opening the black box: Phylogenetics and morphological evolution of the Malagasy fossorial lizards of the subfamily “Scincinae”. Molecular Phylogenetics and Evolution 34: 118–133. <https://doi.org/10.1016/j.ympev.2004.08.016>
- Synave H (1953) Un Cixiide troglobie découvert dans les galeries souterraines du système de Namoroka (Hemiptera – Homoptera). Naturaliste Malgache 5: 175–179.
- Vaillant L (1885) Sur quelques Batraciens de Nossi-Bé (Madagascar), appartenant à la collection du Muséum. Bulletin de la Société Philomathique de Paris (Septième Série) 9: 115–118.
- Vences M, Herrmann C, Multzsch M, Gippner S, Razafimanafa D, Rahagalala NA, Rakotomanga S, Rakotoarison A, Glaw F, Miralles A (2025) Revision of the *Lygodactylus tolampyae* complex, with descriptions of three additional new dwarf gecko species from Madagascar’s North West. Zootaxa 5665: 301–328. <https://doi.org/10.11646/zootaxa.5665.3.1>
- Wilkin P, Rakotonasolo F, Schols P, Furness CA (2002) A new species of *Dioscorea* (Dioscoreaceae) from Western Madagascar and its pollen morphology. Kew Bulletin 57: 901–909. <https://doi.org/10.2307/4115720>
- Wood H (2008) A revision of the assassin spiders of the *Eriauchenius gracilicollis* group, a clade of spiders endemic to Madagascar (Araneae: Archaeidae). Zoological Journal of the Linnean Society 152: 255–296. <https://doi.org/10.1111/j.1096-3642.2007.00359.x>

## Supplementary Material 1

### Files S1, S2

**Authors:** Miralles A, Scherz MD, Hyde Roberts S, Rakotoarison A, Glaw F, Vences M (2026)

**Data type:** .zip

**Explanation notes:** **File S1.** List of specimens examined morphologically [docx file]. — **File S2.** GenBank accession numbers, and localities [docx file].

**Copyright notice:** This dataset is made available under the Open Database License (<http://opendatacommons.org/licenses/odbl/1.0>). The Open Database License (ODbL) is a license agreement intended to allow users to freely share, modify, and use this dataset while maintaining this same freedom for others, provided that the original source and author(s) are credited.

Link: <https://doi.org/10.3897/vz.76.e176241.suppl1>